iScience

CellPress
OPEN ACCESS

Article

Free-standing conductive nickel metal-organic framework nanowires as bifunctional electrodes for wearable pressure sensors and Ni-Zn batteries

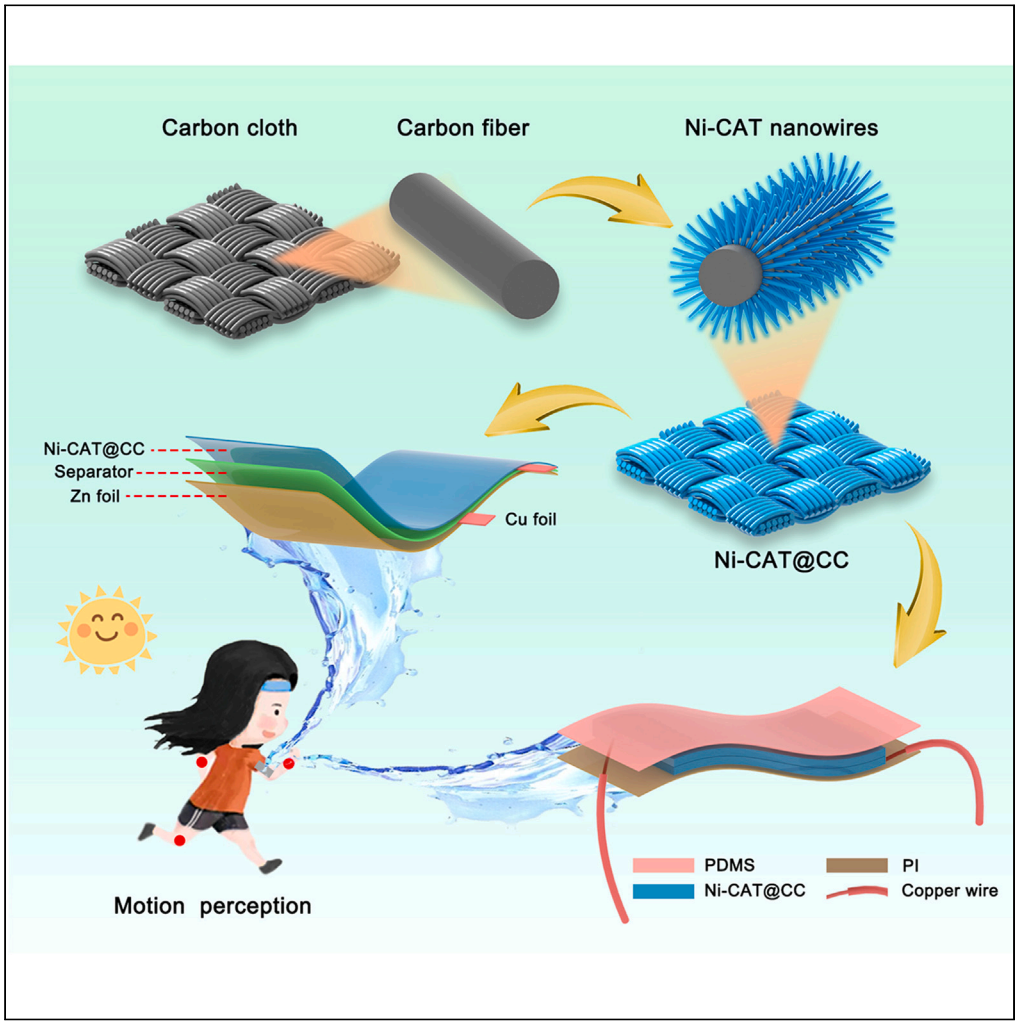

Yuan Fan, Yuanao Zhang, Jiajun Wu, ..., Ming Chen, Qichong Zhang, Qingwen Li

qczhang2016@sinano.ac.cn (Q.Z.)
qwli2007@sinano.ac.cn (Q.L.)

Highlights

The Ni-CAT@CC composite film was prepared by a simple method

MOF-based pressure sensors enable real-time monitoring of human motion

The high potential of using conductive MOFs in wearable applications

Fan et al., iScience 26, 107397
August 18, 2023
https://doi.org/10.1016/j.isci.2023.107397

iScience

CellPress
OPEN ACCESS

Article

Free-standing conductive nickel metal-organic framework nanowires as bifunctional electrodes for wearable pressure sensors and Ni-Zn batteries

Yuan Fan,[1] Yuanao Zhang,[2] Jiajun Wu,[1] Song Zhao,[1] Jiabin Guo,[1] Zhimin Wang,[1] Ming Chen,[3] Qichong Zhang,[1,4,*] and Qingwen Li[1,*]

SUMMARY

Free-standing metal-organic frameworks (MOFs) with controllable structure and good stability are emerging as promising materials for applications in flexible pressure sensors and energy-storage devices. However, the inherent low electrical conductivity of MOF-based materials requires complex preparation processes that involve high-temperature carbonization. This work presents a simple method to grow conductive nickel MOF nanowire arrays on carbon cloth (Ni-CAT@CC) and use Ni-CAT@CC as the functional electrodes for flexible piezoresistive sensor. The resulting sensor is able to monitor human activity, including elbow bending, knee bending, and wrist bending. Besides, the soft-packaged aqueous Ni-Zn battery is assembled with Ni-CAT@CC, a piece of glass microfiber filters, and Zn foil acting as cathode, separator, and anode, respectively. The Ni-Zn battery can be used as a power source for finger pressure monitoring. This work demonstrates free-standing MOF-based nanowires as bifunctional fabric electrodes for wearable electronics.

INTRODUCTION

The development of flexible and wearable sensing devices is of great importance in personal lifestyle and healthcare.[1–3] Among them, flexible pressure sensors are considered to be the most exciting smart sensors due to their extensive fields of application, such as pulse wave monitoring,[4] human motion perception,[5,6] soft robotics,[7] and human-machine interfaces.[8] Piezoresistive sensors, as a type of pressure sensors, have gained much interest on account of their simple structure and easy integration.[9–16] It is generally believed that the material choice and the construction of the device geometry have a significant influence on the performance of piezoresistive sensors as the resistance of the active materials is modulated by changing the geometry of the material when external pressure is applied.[17] Consequently, the development of piezoresistive sensors, from structural design to material selection, remains a major challenge.

To date, smart textiles have been developed for a wide range of wearable devices and have been used to monitor physiological parameters.[18–23] Commercial carbon cloth (CC) is a low-cost textile with high flexibility and good conductivity, which is widely used in flexible supercapacitors and batteries.[24–26] Currently, CC has shown excellent application prospects in the areas of piezoresistive pressure sensing. In a recent example, Chen et al. reported that a flexible piezoresistive pressure sensor based on carbon nanotubes/CC with a high sensitivity ($\approx$120 kPa^{-1}) could monitor human physiological signals.[27] More recently, Wang et al. developed MXene/FeCo alloy@carbon-decorated CC with excellent pressure sensing performance that could be used for human motion perception.[28] Thus, it is highly desirable to fabricate the piezoresistive pressure sensor by using CC as a flexible substrate.

Metal-organic frameworks (MOFs), also known as porous coordination polymers, have been explored for a number of applications including energy conversion and storage,[29] triboelectric nanogenerators,[30–32] catalysis,[33] and thermoelectric.[34,35] With the merits of reliable host-guest interactions and responsiveness to chemical stimuli, MOFs have attracted increasing interest in the field of electronic sensors.[36] To pursue broader applications, recent studies have focused on MOFs materials as promising candidates for piezoresistive pressure sensors. For instance, Zhao et al. reported a flexible piezoresistive sensor based on MOF-derived porous carbon and polydimethylsiloxane (PDMS) composite, which was obtained by carbonization

[1]Key Laboratory of Multifunctional Nanomaterials and Smart Systems, Suzhou Institute of Nano-Tech and Nano-Bionics, Chinese Academy of Sciences, Suzhou 215123, China

[2]Department of Nano Science and Technology Institute, University of Science and Technology of China, Suzhou 215123, China

[3]Shenzhen Institute of Advanced Technology, Chinese Academy of Sciences, Shenzhen 518055, China

[4]Lead contact

*Correspondence: qczhang2016@sinano.ac.cn (Q.Z.), qwli2007@sinano.ac.cn (Q.L.)

https://doi.org/10.1016/j.isci.2023.107397

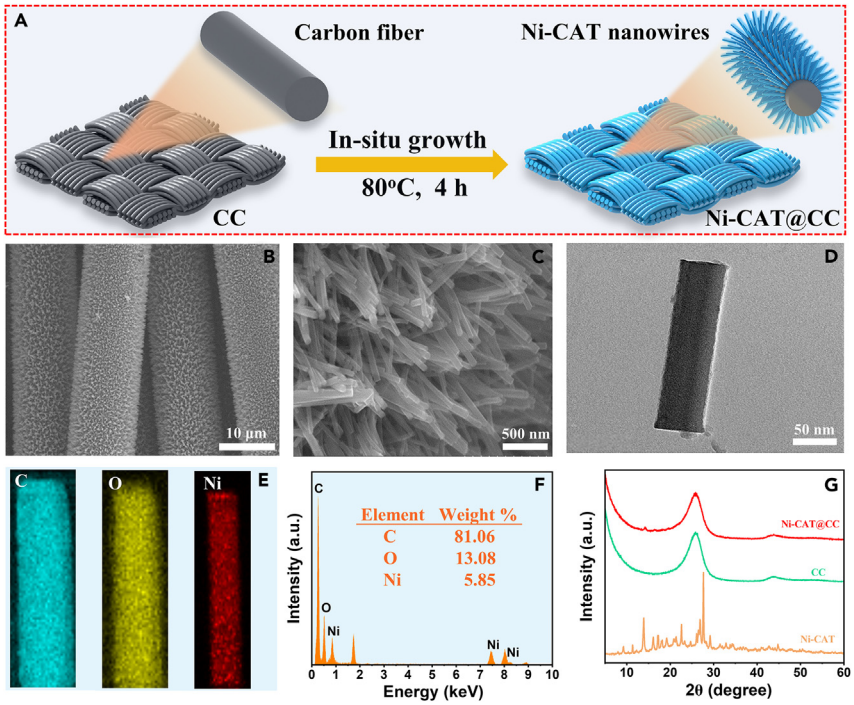

Figure 1. Microstructural and chemical characterizations

(A) Schematic illustration of the preparation of Ni-CAT@CC composite film.

(B and C) SEM images of Ni-CAT@CC at different magnifications.

(D and E) TEM image of Ni-CAT (D) with corresponding EDX elemental mapping (E).

(F) EDX spectra of Ni-CAT.

(G) XRD patterns of the Ni-CAT powder, pristine CC, and Ni-CAT@CC.

and acid etching of MOF-5 and then mechanical mixing with PDMS.[37] It showed excellent properties for pressure sensing and could detect human motions. Wang et al. investigated carbonized zeolitic imidazole framework-8 (ZIF-8) and polyaniline nanofiber on polyurethane sponge to assemble a flexible piezoresistive sensor with a high sensitivity that could monitor human motions.[38] However, these MOF-based materials suffer from complicated fabrication processes that usually require high-temperature carbonization to improve their electrical conductivity, which increases the cost. As a result, there is a need to simplify the fabrication process of MOF-based materials as flexible pressure sensors.

Due to their intrinsic electrical conductivities and periodic porous structures, conductive MOFs as the active materials provide a promising way for the fabrication of piezoresistive pressure sensors.[39,40] For example, Zhou et al. reported conductive $Cu_3(HHTP)_2$ MOF into a well-aligned MOF hybrid array on copper mesh for flexible pressure sensor and applied to monitor the human pulse and finger motion.[39] In this paper, we demonstrate a conductive MOF, nickel triphenylene-fused metal catecholate (Ni-CAT), as active materials for the fabrication of MOF-based piezoresistive pressure sensor by a simple hydrothermal method. Ni-CAT nanowires were in situ grown on the surface of CC (denoted as Ni-CAT@CC), and it has succeeded to be assembled as flexible pressure sensor. This sensor has a moderate response/recovery time and good stability and can also monitor human motions. Furthermore, we have explored the soft-packaged aqueous Ni-Zn battery, in which the Ni-CAT@CC, glass microfiber filters, and Zn foil serve as the cathode, separator, and anode, respectively. It can be used as a power source for finger pressure monitoring. Totally, this design concept of a bifunctional, lightweight, and flexible textile can be used not only for flexible piezoresistive pressure sensors but also for Ni-Zn battery, showing high potential for wearable applications.

RESULTS

Preparation and characterization

The preparation process of the Ni-CAT@CC composite is schematically illustrated in Figure 1A. The structure of MOF nanowires on CC was synthesized by hydrothermal method. In particular, to improve the

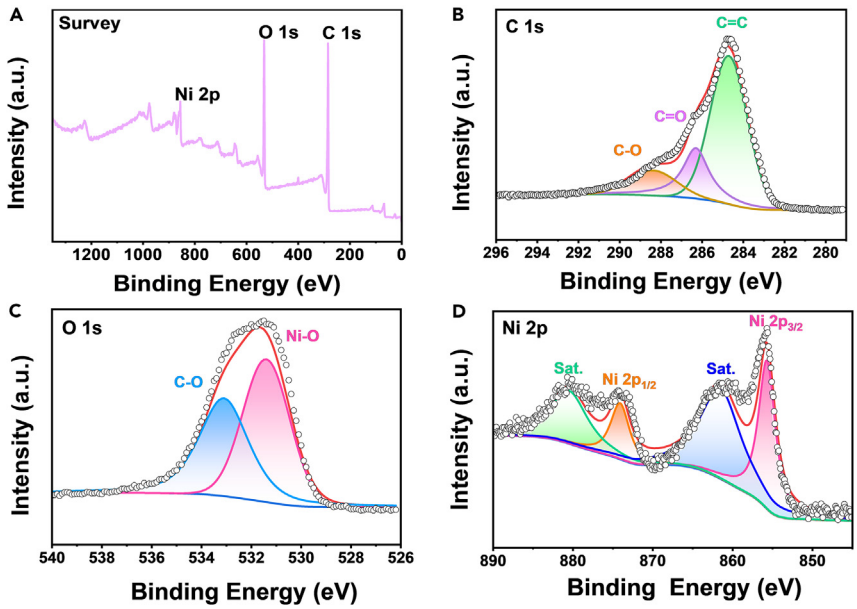

Figure 2. XPS spectra of Ni-CAT@CC sample

(A) XPS survey scan of Ni-CAT@CC.

(B) XPS spectra of C 1s regions of Ni-CAT@CC.

(C) XPS spectra of O 1s regions of Ni-CAT@CC.

(D) XPS spectra of Ni 2P regions of Ni-CAT@CC.

hydrophilicity of the CC, we chose the oxygen plasma treatment before use. The oxygen plasma-treated CC was added with homogeneous solution composed of the Ni(II) and 2,3,6,7,10,11-hexahydroxytriphenylene (HHTP) ligands prior to forming a Ni-CAT@CC composite film. The sensors were prepared as follows: the two layers of Ni-CAT@CC (2 × 2 cm^2) were stacked, and the top and bottom layers were bonded to copper wires with copper foils. Finally, the sensor was encapsulated using PDMS film as the top layer and polyimide tape as the bottom layer to ensure that the Ni-CAT@CC-based sensor is flexible and durable.

As shown in Figure 1B, the uniform coverage of Ni-CAT nanowires on the CC was observed by scanning electron microscopy (SEM). Due to the hydrophilic CC substrate, numerous Ni-CAT nanowires were epitaxially grown out from the CC substrate surface (Figure 1C), which is beneficial to the large number of point faces contacting between the Ni-CAT@CC and PDMS film. The structure and composition of the Ni-CAT@CC composite film were measured by transmission electron microscopy (TEM) and energy dispersive X-ray (EDX) spectroscopy, as shown in Figures 1D–1F. In Figure 1D, the TEM image of the Ni-CAT (removed from the Ni-CAT@CC surface) shows the structure of the nanowire. The corresponding EDX images suggest the homogeneous distribution of C, O, and Ni elements (Figure 1E), and the signal for Ni content was 5.85%, confirming the successful growth of Ni-CAT on CC (Figure 1F). The X-ray diffractometer (XRD) patterns of Ni-CAT powder, pristine CC, and Ni-CAT@CC are shown in Figure 1G. The peaks observed in the XRD pattern of Ni-CAT powder were in good agreement with those previously reported.[41,42] The diffraction peaks at $2\theta = 26°$ and 44° show the typical peaks of the pristine CC, which were assigned to the (002) and (100) planes of amorphous carbon.[25] The characteristic peak at 14.2° appeared in Ni-CAT@CC, further demonstrating the successful preparation of Ni-CAT grown on the surface of CC.

The surface chemical states of Ni-CAT@CC composite film are further examined by X-ray photoelectron spectroscopy (XPS), which clearly displays the three signals of C, O, and Ni elements (Figure 2A). This result further indicates the presence of the Ni element in Ni-CAT@CC, which is in accordance with the result of the EDX mapping. As shown in Figure 2B, the C 1s XPS spectrum of Ni-CAT@CC could be fitted into three peaks at ≈284.7, ≈286.3, and ≈288.4 eV, which were attributed to C=C, C=O, and C-O, respectively.[43] The O 1s XPS spectrum displayed two peaks at ≈531.4 and ≈533.1 eV (Figure 2C), which corresponded

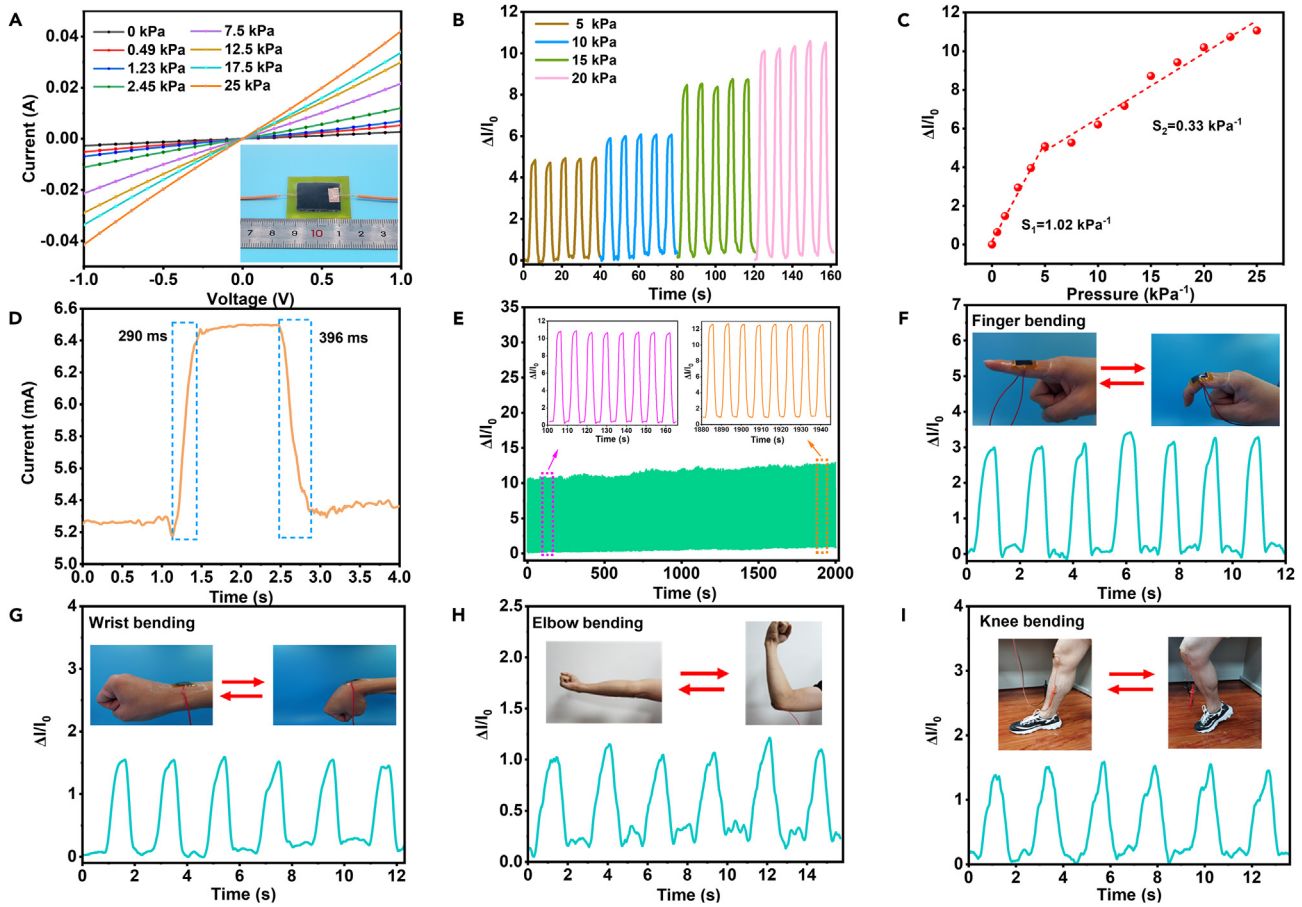

Figure 3. Performance of the Ni-CAT@CC-based piezoresistive pressure sensor

(A) I-V curves of the Ni-CAT@CC sensor device under different applied pressures.

(B) I-T curves of the Ni-CAT@CC-based sensor response under different pressures.

(C) Sensitivity curve of the Ni-CAT@CC-based sensor.

(D) Response/recovery time of Ni-CAT@CC-based pressure sensor under 15 kPa.

(E) Stability test of the device.

(F–I) Application tests of Ni-CAT@CC-based sensor for real-time human activity monitoring including finger bending (F), wrist bending (G), elbow bending (H), and knee bending (I) are shown in the form of I-T curves.

to Ni-O and C-O, respectively.[43] The Ni 2p region (Figure 2D) exhibited two main peaks at 855.7 and 874.1 eV, which were related to the Ni $2p_{3/2}$ and Ni $2p_{1/2}$ of Ni(II), respectively.[43,44] Taken together, these results indicate the successful synthesis of the Ni-CAT@CC composite film.

Sensing properties of Ni-CAT@CC-based sensor

The principle of piezoresistive pressure sensors is based on the piezoresistive effect, that is, the change in resistance of a material when stimulated by an applied pressure.[45] Piezoresistive pressure sensors are able to detect pressure by means of the changes in resistance of devices when they are deformed.[46] The sensing properties of the Ni-CAT@CC-based piezoresistive sensors were studied. Figure 3A presents the current-voltage curves of the assembled sensor, which vary from −1.0 to 1.0 V at different pressures, and the inset of Figure 3A displays the photo of the flexible piezoresistive pressure sensor based on Ni-CAT@CC composite. Apparently, a good linear relationship of all the curves was observed, and an increase of the curve slope was obtained by increasing the pressure, suggesting a good ohmic contact.[47] As revealed in Figure 3B, the rate of current variation increased as the pressure increased. The Ni-CAT@CC-based sensor possesses the ability to detect different pressures and has a stable response. Sensitivity (S) is a key parameter and can be expressed as $S = (\Delta I/I_0)/\Delta P$, where ΔI represents the relative change in current, I_0 means the initial current

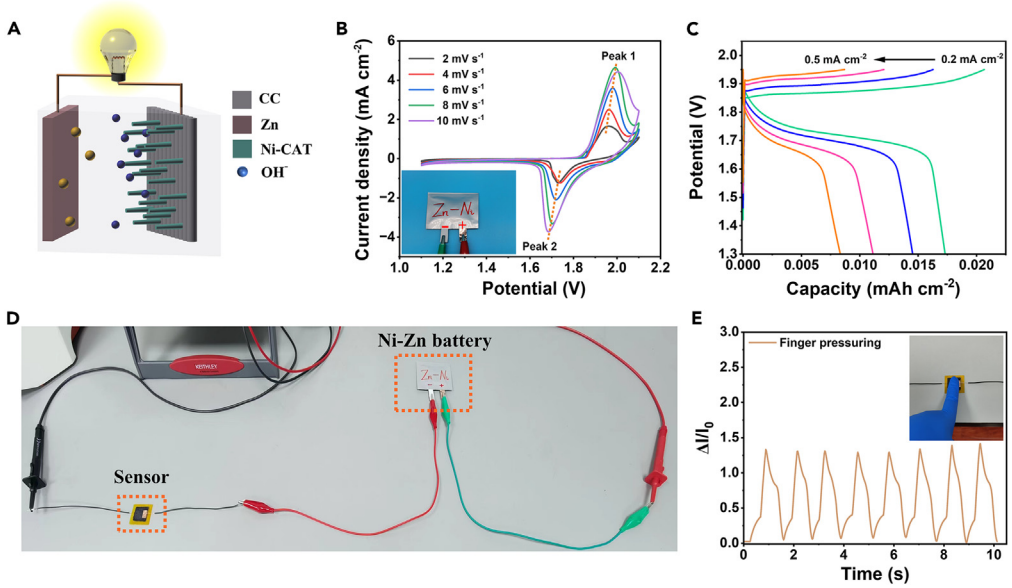

Figure 4. Electrochemical performances of Ni-CAT@CC-based soft-packaged aqueous Ni-Zn battery

(A) Schematic of Ni-Zn battery based on metallic Zn and Ni-CAT@CC cathode.

(B) CV curves of as-assembled Ni//Zn battery at various scan rates.

(C) GCD curves of as-assembled Ni//Zn battery at different current densities.

(D) The digital images of the integrated system where the Ni-CAT@CC based sensor was connected to the Ni//Zn battery.

(E) Detection of finger touch powered by Ni//Zn battery.

without pressure, and ΔP is the relative change in pressure.[6] Figure 3C depicts the sensitivity curve of Ni-CAT@CC-based sensor. The S of this device was 1.02 kPa^{-1} in a pressure range of 0–5 kPa and 0.33 kPa^{-1} in the range of 5–25 kPa. The results reveal that the value of S decreases with external load. The reason should be that the flexible Ni-CAT@CC layer initially deforms as the applied pressure increases. When pressure was applied to the sensor surface, the plane-to-plane contact area increased and more conductive paths were formed, resulting in lower resistance.[48] As the pressure continued to increase, the contact points of the Ni-CAT@CC were in close contact and the conductive paths reached saturation, leading to resistance changes with lower sensitivity.[27] Figure 3D shows the real-time response curve of the Ni-CAT@CC-based sensor. As can be seen, the response/recovery time is 290/396 ms under the force of 15 kPa, which is applicable to monitor human motion.[49,50] As shown in Figure 3E, the sensor shows good stability during the 2,000 s test under 20 kPa, indicating the mechanical robustness with good potential for applications. Moreover, tests were carried out by attaching the sensor to joints of the human body using a piece of medical scotch tape and collecting real-time motion signals of human fingers, wrists, elbows, and knees (Figures 3F–3I). The results show that the sensor can recognize different human activities by comparing shape and intensity. Overall, the good stability and moderate response/recovery time make it an ideal wearable device that can detect real-time motion signals of different parts of the human body.

Electrochemical properties of Ni-CAT@CC-based Ni-Zn battery

The schematic of the soft-packaged battery was assembled as shown in Figure 4A, using the activated Ni-CAT@CC composite film as the cathode, Zn foil as the anode, and 1 M KOH as the aqueous electrolyte. The inset of Figure 4B shows the digital image of the soft-packaged aqueous Ni-Zn battery encapsulated by aluminum plastic film. Figure 4B displays the cyclic voltammetry (CV) curves of the assembled battery recorded at scan rates between 2 and 10 mV s^{-1}. Notably, all the curves have strong pairs of redox peaks in the potential window between 1.1 and 2.1 V, suggesting the typical battery-type electrochemical behavior.[51] The galvanostatic charge-discharge (GCD) curves of the soft-packaged battery were recorded at different current densities, as shown in Figure 4C. The discharge capacity of 0.017 mA h cm^{-2} was obtained at low current density, whereas as the current density increased to 0.5 mA cm^{-2}, the discharge capacity decreased to 0.008 mA h cm^{-2}. At the same time, the cycling performance of the Ni//Zn battery was also tested, as shown in Figure S1. It was found that the capacity of the Ni//Zn battery remained 76% after

100 cycles. The charging and discharging behavior of Ni-CAT@CC at a current density of 0.3 mA cm^{-2} was also investigated (Figure S2A), and the corresponding high-resolution Ni 2p XPS spectra of Ni-CAT@CC at different charging/discharging states are shown in Figures S2B–S2F. The electrochemical conversion between Ni^{2+} and Ni^{3+} was demonstrated, similar to that previously reported for the Ni-MOF.[44,51] Considering the practical applications in wearable devices, a simple integration system was designed. As shown in Figure 4D, a Ni-CAT@CC-based sensor was connected to a Ni-CAT@CC-based cell, and the cell was used as the power source. Meanwhile, by connecting the sensor to a source meter (Keithley 2450), a test system is formed. Figure 4E depicts the response of the Ni-CAT@CC-based sensor to finger touch. Finger touch can be detected when the sensor is pressed with a finger, proving that the dual-function Ni-CAT@CC can be used not only as a sensor but also as a self-powered device.

DISCUSSION

In summary, the Ni-CAT@CC was synthesized by employing a facile and effective method, and the Ni-CAT@CC-based pressure sensor was assembled. Taking advantage of the integrated benefits of the moderate response/recovery time, wide linear ranges, and good stability, we explored the practical application of the fabricated sensor to monitor human activity in real time. In addition, the Ni-CAT@CC composite film was also used as a cathode to develop a soft-packaged aqueous Ni-Zn battery as well. The assembled Ni-Zn battery was used as a power source for the Ni-CAT@CC-based pressure sensor, providing an excellent template for the fabrication of multifunctional wearable devices.

Limitations of the study

The construction of a flexible, free-standing composite film using CC and 2D conductive MOF provides a simple method and feasible solution for the fabrication of the piezoresistive sensors. The conductive MOF serves as the active component to sense the external pressure. However, the Ni-CAT@CC-based piezoresistive sensors lack high sensitivity and fast response time, which has limited their applications to sensing the very low to high pressure range. The design and fabrication of high-performance materials for both sensing and energy storage will be a major focus of future research. We expect multifunctional materials to play an important role in wearable electronic devices.

STAR★METHODS

Detailed methods are provided in the online version of this paper and include the following:

- KEY RESOURCES TABLE
- RESOURCE AVAILABILITY
  - Lead contact
  - Materials availability
  - Data and code availability
- METHOD DETAILS
  - Preparation of Ni-CAT@CC composite
  - Assembly of piezoresistive sensor based on Ni-CAT@CC
  - Fabrication and assembly of the soft-packaged aqueous Ni-Zn battery
  - Characterization and measurement

SUPPLEMENTAL INFORMATION

Supplemental information can be found online at https://doi.org/10.1016/j.isci.2023.107397.

ACKNOWLEDGMENTS

This work was supported by the Natural Science Foundation of Jiangsu Province (BK20220288), Suzhou Institute of Nano-Tech and Nano-Bionics, Chinese Academy of Sciences (Start-up grant E1552102). Y. F. acknowledges the support of Jiangsu Funding Program for Excellent Postdoctoral Talent.

AUTHOR CONTRIBUTIONS

Conceptualization, Investigation, Data curation, Writing – Original Draft, Y. F.; Characterization, Y. Z., J. W., S. Z.; Methodology, J. G., Z. W.; Resources, M. C.; Supervision, Funding Acquisition, Q. Z. and Q. L.

DECLARATION OF INTERESTS

The authors declare no competing interests.

INCLUSION AND DIVERSITY

We support inclusive, diverse, and equitable conduct of research.

Received: March 14, 2023
Revised: June 19, 2023
Accepted: July 11, 2023
Published: July 13, 2023

REFERENCES

1. Pyo, S., Lee, J., Bae, K., Sim, S., and Kim, J. (2021). Recent progress in flexible tactile sensors for human-interactive systems: from sensors to advanced applications. Adv. Mater. *33*, 2005902. https://doi.org/10.1002/adma.202005902.

2. Wang, L., Li, N., Zhang, Y., Di, P., Li, M., Lu, M., Liu, K., Li, Z., Ren, J., Zhang, L., and Wan, P. (2022). Flexible multiresponse-actuated nacre-like MXene nanocomposite for wearable human-machine interfacing. Matter *5*, 3417–3431. https://doi.org/10.1016/j.matt.2022.06.052.

3. Li, J., Liu, Y., Yuan, L., Zhang, B., Bishop, E.S., Wang, K., Tang, J., Zheng, Y.Q., Xu, W., Niu, S., et al. (2022). A tissue-like neurotransmitter sensor for the brain and gut. Nature *606*, 94–101. https://doi.org/10.1038/s41586-022-04615-2.

4. Meng, K., Xiao, X., Wei, W., Chen, G., Nashalian, A., Shen, S., Xiao, X., and Chen, J. (2022). Wearable pressure sensors for pulse wave monitoring. Adv. Mater. *34*, 2109357. https://doi.org/10.1002/adma.202109357.

5. Hou, Y., Wang, L., Sun, R., Zhang, Y., Gu, M., Zhu, Y., Tong, Y., Liu, X., Wang, Z., Xia, J., et al. (2022). Crack-across-pore enabled high-performance flexible pressure sensors for deep neural network enhanced sensing and human action recognition. ACS Nano *16*, 8358–8369. https://doi.org/10.1021/acsnano.2c02609.

6. Yin, T., Cheng, Y., Hou, Y., Sun, L., Ma, Y., Su, J., Zhang, Z., Liu, N., Li, L., and Gao, Y. (2022). 3D porous structure in MXene/PANI foam for a high-performance flexible pressure sensor. Small *18*, 2204806. https://doi.org/10.1002/smll.202204806.

7. Zhang, Y., Yang, J., Hou, X., Li, G., Wang, L., Bai, N., Cai, M., Zhao, L., Wang, Y., Zhang, J., et al. (2022). Highly stable flexible pressure sensors with a quasi-homogeneous composition and interlinked interfaces. Nat. Commun. *13*, 1317. https://doi.org/10.1038/s41467-022-29093-y.

8. Guo, Y., Zhong, M., Fang, Z., Wan, P., and Yu, G. (2019). A wearable transient pressure sensor made with MXene nanosheets for sensitive broad-range human-machine interfacing. Nano Lett. *19*, 1143–1150. https://doi.org/10.1021/acs.nanolett.8b04514.

9. Guo, Y., Guo, Z., Zhong, M., Wan, P., Zhang, W., and Zhang, L. (2018). A flexible wearable pressure sensor with bioinspired microcrack and interlocking for full-range human-machine interfacing. Small *14*, 1803018. https://doi.org/10.1002/smll.201803018.

10. Liu, W., Liu, N., Yue, Y., Rao, J., Cheng, F., Su, J., Liu, Z., and Gao, Y. (2018). Piezoresistive pressure sensor based on synergistical innerconnect polyvinyl alcohol nanowires/wrinkled graphene film. Small *14*, 1704149. https://doi.org/10.1002/smll.201704149.

11. Yu, R., Xia, T., Wu, B., Yuan, J., Ma, L., Cheng, G.J., and Liu, F. (2020). Highly sensitive flexible piezoresistive sensor with 3D conductive network. ACS Appl. Mater. Interfaces *12*, 35291–35299. https://doi.org/10.1021/acsami.0c09552.

12. Yang, T., Deng, W., Chu, X., Wang, X., Hu, Y., Fan, X., Song, J., Gao, Y., Zhang, B., Tian, G., et al. (2021). Hierarchically microstructure-bioinspired flexible piezoresistive bioelectronics. ACS Nano *15*, 11555–11563. https://doi.org/10.1021/acsnano.1c01606.

13. Cao, K., Wu, M., Bai, J., Wen, Z., Zhang, J., Wang, T., Peng, M., Liu, T., Jia, Z., Liang, Z., and Jiang, L. (2022). Beyond skin pressure sensing: 3D printed laminated graphene pressure sensing material combines extremely low detection limits with wide detection range. Adv. Funct. Mater. *32*, 2202360. https://doi.org/10.1002/adfm.202202360.

14. Zheng, X., Wang, P., Zhang, X., Hu, Q., Wang, Z., Nie, W., Zou, L., Li, C., and Han, X. (2022). Breathable, durable and bark-shaped MXene/textiles for high-performance wearable pressure sensors, EMI shielding and heat physiotherapy. Composites Part A *152*, 106700. https://doi.org/10.1016/j.compositesa.2021.106700.

15. Wang, H., Tao, J., Jin, K., Wang, X., and Dong, Y. (2022). Multifunctional pressure/temperature/bending sensor made of carbon fibre-multiwall carbon nanotubes for artificial electronic application. Composites Part A *154*, 106796. https://doi.org/10.1016/j.compositesa.2021.106796.

16. Song, S., Zhang, C., Li, W., Wang, J., Rao, P., Wang, J., Li, T., and Zhang, Y. (2022). Bioinspired engineering of gradient and hierarchical architecture into pressure sensors toward high sensitivity within ultra-broad working range. Nano Energy *100*, 107513. https://doi.org/10.1016/j.nanoen.2022.107513.

17. Wang, Y., Yue, Y., Cheng, F., Cheng, Y., Ge, B., Liu, N., and Gao, Y. (2022). $Ti_3C_2T_x$ MXene-based flexible piezoresistive physical sensors. ACS Nano *16*, 1734–1758. https://doi.org/10.1021/acsnano.1c09925.

18. Libanori, A., Chen, G., Zhao, X., Zhou, Y., and Chen, J. (2022). Smart textiles for personalized healthcare. Nat. Electron. *5*, 142–156. https://doi.org/10.1038/s41928-022-00723-z.

19. Xu, R., She, M., Liu, J., Zhao, S., Liu, H., Qu, L., and Tian, M. (2022). Breathable kirigami-shaped ionotronic e-textile with touch/strain sensing for friendly epidermal electronics. Adv. Fiber Mater. *4*, 1525–1534. https://doi.org/10.1007/s42765-022-00186-z.

20. Wen, D.L., Pang, Y.X., Huang, P., Wang, Y.L., Zhang, X.R., Deng, H.T., and Zhang, X.S. (2022). Silk fibroin-based wearable all-fiber multifunctional sensor for smart clothing. Adv. Fiber Mater. *4*, 873–884. https://doi.org/10.1007/s42765-022-00150-x.

21. Wang, J., Xu, S., Zhang, C., Yin, A., Sun, M., Yang, H., Hu, C., and Liu, H. (2023). Field effect transistor-based tactile sensors: from sensor configurations to advanced applications. InfoMat *5*, 12376. https://doi.org/10.1002/inf2.12376.

22. Yu, Y., Guo, J., Zhang, H., Wang, X., Yang, C., and Zhao, Y. (2022). Shear-flow-induced graphene coating microfibers from microfluidic spinning. The Innovation *3*, 100209. https://doi.org/10.1016/j.xinn.2022.100209.

23. Chen, M., Liu, J., Li, P., Gharavi, H., Hao, Y., Ouyang, J., Hu, J., Hu, L., Hou, C., Humar, I., et al. (2022). Fabric computing: concepts, opportunities, and challenges. Innovation *3*, 100340. https://doi.org/10.1016/j.xinn.2022.100340.

24. Meng, S., Liang, J., Jia, W., Zhang, P., Su, Q., Wang, C., An, L., Chen, L., and Wang, Y. (2022). Metal-free and flexible surface-enhanced Raman scattering substrate based on oxidized carbon cloth. Carbon *189*, 152–161. https://doi.org/10.1016/j.carbon.2021.12.055.

25. Wang, Q., Wang, Y., Zhang, T., Wang, Y., Zhang, Q., Li, T., and Han, Y. (2022). Electrochemical polymerization of polypyrrole on carbon cloth@ZIF67 using alizarin red S as redox dopant for flexible supercapacitors. Electrochim. Acta *407*, 139869. https://doi.org/10.1016/j.electacta.2022.139869.

26. Wang, Y., Yang, H., Lv, H., Zhou, Z., Zhao, Y., Wei, H., and Chen, Z. (2022). High performance flexible asymmetric supercapacitor constructed by cobalt aluminum layered double hydroxide @ nickel cobalt layered double hydroxide heterostructure grown in-situ on carbon cloth. J. Colloid Interface Sci. *610*, 35–48. https://doi.org/10.1016/j.jcis.2021.12.019.

27. Chen, D., Zhang, T., Geng, W., Sun, D., Liu, X., Li, Y., Liu, H., and Zhou, W. (2022). An intelligent tactile sensor based on interlocked carbon nanotube array for ultrasensitive physiological signal detection and rea-time monitoring. Adv. Mater. Technol. *7*, 2200290. https://doi.org/10.1002/admt.202200290.

28. Wang, S., Li, D., Jiang, L., and Fang, D. (2022). Flexible and mechanically strong MXene/FeCo@C decorated carbon cloth: A multifunctional electromagnetic interference shielding material. Compos. Sci. Technol. *221*, 109337. https://doi.org/10.1016/j.compscitech.2022.109337.

29. Bai, Y., Liu, C., Shan, Y., Chen, T., Zhao, Y., Yu, C., and Pang, H. (2022). Metal-organic frameworks nanocomposites with different dimensionalities for energy conversion and storage. Adv. Energy Mater. *12*, 2100346. https://doi.org/10.1002/aenm.202100346.

30. Khandelwal, G., Maria Joseph Raj, N.P., and Kim, S.J. (2020). Zeolitic imidazole framework: metal–organic framework subfamily members for triboelectric nanogenerators. Adv. Funct. Mater. *30*, 1910162. https://doi.org/10.1002/adfm.201910162.

31. Rahman, M.T., Rana, S.S., Zahed, M.A., Lee, S., Yoon, E.S., and Park, J.Y. (2022). Metal-organic framework-derived nanoporous carbon incorporated nanofibers for high-performance triboelectric nanogenerators and self-powered sensors. Nano Energy *94*, 106921. https://doi.org/10.1016/j.nanoen.2022.106921.

32. Hajra, S., Sahu, M., Sahu, R., Padhan, A.M., Alagarsamy, P., Kim, H.G., Lee, H., Oh, S., Yamauchi, Y., and Kim, H.J. (2022). Significant effect of synthesis methodologies of metal-organic frameworks upon the additively manufactured dual-mode triboelectric nanogenerator towards self-powered applications. Nano Energy *98*, 107253. https://doi.org/10.1016/j.nanoen.2022.107253.

33. Ye, G., Wan, L., Zhang, Q., Liu, H., Zhou, J., Wu, L., Zeng, X., Wang, H., Chen, X., and Wang, J. (2023). Boosting catalytic performance of MOF-808(Zr) by direct generation of rich defective Zr nodes via a solvent-free approach. Inorg. Chem. *62*, 4248–4259. https://doi.org/10.1021/acs.inorgchem.2c04364.

34. Fan, Y., Liu, Z., and Chen, G. (2021). Recent progress in designing thermoelectric metal-organic frameworks. Small *17*, 2100505. https://doi.org/10.1002/smll.202100505.

35. Fan, Y., Liu, Z., and Chen, G. (2022). Constructing flexible metal-organic framework/polymer/carbon nanotubes ternary composite films with enhanced thermoelectric properties for heat-to-electricity conversion. Compos. Commun. *29*, 100997. https://doi.org/10.1016/j.coco.2021.100997.

36. Zhang, L.T., Zhou, Y., and Han, S.T. (2021). The role of metal-organic frameworks in electronic sensors. Angew. Chem. Int. Ed. *60*, 15192–15212. https://doi.org/10.1002/anie.202006402.

37. Zhao, X.H., Ma, S.N., Long, H., Yuan, H., Tang, C.Y., Cheng, P.K., and Tsang, Y.H. (2018). Multifunctional sensor based on porous carbon derived from metal-organic frameworks for real time health monitoring. ACS Appl. Mater. Interfaces *10*, 3986–3993. https://doi.org/10.1021/acsami.7b16859.

38. Wang, Y., Chao, M., Wan, P., and Zhang, L. (2020). A wearable breathable pressure sensor from metal-organic framework derived nanocomposites for highly sensitive broad-range healthcare monitoring. Nano Energy *70*, 104560. https://doi.org/10.1016/j.nanoen.2020.104560.

39. Zhou, K., Zhang, C., Xiong, Z., Chen, H.Y., Li, T., Ding, G., Yang, B., Liao, Q., Zhou, Y., and Han, S.T. (2020). Template-directed growth of hierarchical MOF hybrid arrays for tactile sensor. Adv. Funct. Mater. *30*, 2001296. https://doi.org/10.1002/adfm.202001296.

40. Zhao, Y., Hou, N., Wang, Y., Fu, C., Li, X., Li, L., and Zhang, W. (2022). All-fiber structure covered with two-dimensional conductive MOF materials to construct a comfortable, breathable and high-quality self-powered wearable sensor system. J. Mater. Chem. A *10*, 1248–1256. https://doi.org/10.1039/D1TA08453D.

41. Hmadeh, M., Lu, Z., Liu, Z., Gándara, F., Furukawa, H., Wan, S., Augustyn, V., Chang, R., Liao, L., Zhou, F., et al. (2012). New porous crystals of extended metal-catecholates. Chem. Mater. *24*, 3511–3513. https://doi.org/10.1021/cm301194a.

42. Yoon, H., Lee, S., Oh, S., Park, H., Choi, S., and Oh, M. (2019). Synthesis of bimetallic conductive 2D metal-organic framework (Co_xNi_y-CAT) and its mass production: enhanced electrochemical oxygen reduction activity. Small *15*, 1805232. https://doi.org/10.1002/smll.201805232.

43. Shi, Y.X., Wu, Y., Wang, S.Q., Zhao, Y.Y., Li, T., Yang, X.Q., and Zhang, T. (2021). Soft electrochemical actuators with a two-dimensional conductive metal-organic framework nanowire array. J. Am. Chem. Soc. *143*, 4017–4023. https://doi.org/10.1021/jacs.1c00666.

44. Lan, X., Zhang, X., Feng, Y., Yin, S., Xu, J., Wang, X., Xu, Z., Kong, S., Ma, Z., Yong, Z., et al. (2022). Structural engineering of metal-organic frameworks cathode materials toward high-performance flexible aqueous rechargeable Ni–Zn batteries. Mater. Today Energy *30*, 101157. https://doi.org/10.1016/j.mtener.2022.101157.

45. Wan, Y., Wang, Y., and Guo, C.F. (2017). Recent progresses on flexible tactile sensors. Materials Today Physics *1*, 61–73. https://doi.org/10.1016/j.mtphys.2017.06.002.

46. Tang, R., Lu, F., Liu, L., Yan, Y., Du, Q., Zhang, B., Zhou, T., and Fu, H. (2021). Flexible pressure sensors with microstructures. Nano Select *2*, 1874–1901. https://doi.org/10.1002/nano.202100003.

47. Su, T., Liu, N., Lei, D., Wang, L., Ren, Z., Zhang, Q., Su, J., Zhang, Z., and Gao, Y. (2022). Flexible MXene/bacterial cellulose film sound detector based on piezoresistive sensing mechanism. ACS Nano *16*, 8461–8471. https://doi.org/10.1021/acsnano.2c03155.

48. Han, F., Luo, J., Pan, R., Wu, J., Guo, J., Wang, Y., Wang, L., Liu, M., Wang, Z., Zhou, D., et al. (2022). Vanadium dioxide nanosheets supported on carbonized cotton fabric as bifunctional textiles for flexible pressure sensors and zinc-ion batteries. ACS Appl. Mater. Interfaces *14*, 41577–41587. https://doi.org/10.1021/acsami.2c10679.

49. Wang, L., Zhang, M., Yang, B., Tan, J., and Ding, X. (2020). Highly compressible, thermally stable, light-weight, and robust aramid nanofibers/Ti_3AlC_2 MXene composite aerogel for sensitive pressure sensor. ACS Nano *14*, 10633–10647. https://doi.org/10.1021/acsnano.0c04888.

50. Chen, T., Wu, G., Panahi-Sarmad, M., Wu, Y., Xu, R., Cao, S., and Xiao, X. (2022). A novel flexible piezoresistive sensor using superelastic fabric coated with highly durable SEBS/TPU/CB/CNF nanocomposite for detection of human motions. Compos. Sci. Technol. *227*, 109563. https://doi.org/10.1016/j.compscitech.2022.109563.

51. Li, C., Zhang, Q., Li, T., He, B., Man, P., Zhu, Z., Zhou, Z., Wei, L., Zhang, K., Hong, G., and Yao, Y. (2020). Nickel metal–organic framework nanosheets as novel binder-free cathode for advanced fibrous aqueous rechargeable Ni–Zn battery. J. Mater. Chem. A. *8*, 3262–3269. https://doi.org/10.1039/C9TA11136K.

52. Wang, S., Liu, M., Shi, Y., Yang, X., Li, L., Lu, Q., Zheng, H., Feng, S., Bai, Y., and Zhang, T. (2022). Vertically aligned conductive metal-organic framework nanowires array composite fiber as efficient solid-contact for wearable potentiometric sweat sensing. Sensor. Actuator. B Chem. *369*, 132290. https://doi.org/10.1016/j.snb.2022.132290.

STAR★METHODS

KEY RESOURCES TABLE

REAGENT or RESOURCE	SOURCE	IDENTIFIER
Chemicals, peptides, and recombinant proteins		
Nickel(II) acetate tetrahydrate	Aladdin	CAS:6018-89-9
2,3,6,7,10,11-Hexahydroxytriphenylene hydrate	Aladdin	CAS:4877-80-9
Potassium hydroxide	Aladdin	CAS:1310-58-3
Software and algorithms		
Origin 2023	OriginLab	https://www.originlab.com
3ds Max 2021	Autodesk	http://www.autodesk.com

RESOURCE AVAILABILITY

Lead contact

Further information and requests for resources and reagents should be directed to and will be fulfilled by the lead contact, Qichong Zhang (qczhang2016@sinano.ac.cn).

Materials availability

This work did not generate new unique reagents.

Data and code availability

- All data reported in this paper will be shared by the lead contact upon request.
- This paper does not report original code.
- Any additional information required to reanalyze the data reported in this paper is available from the lead contact upon reasonable request.

METHOD DETAILS

Preparation of Ni-CAT@CC composite

First, the CC was placed in a 50 mL beaker and ultrasonicated with anhydrous ethanol and deionized water for 5 min, respectively. Then, the CC was washed with deionized water and dried in an oven at 60 °C overnight. Next, the cleaned CC was treated with an oxygen plasma generator (100 W) for 20 min to obtain more hydrophilic surface. Simultaneously, the Ni-CAT nanowires were prepared according to previously reported method with few modifications.[42,52] Briefly, 0.02 g $Ni(OAc)_2 \cdot 4H_2O$ was added into a 20 mL vessel, and then 0.014 g 2,3,6,7,10,11-hexahydroxytriphenylene hydrate was added into the vessel. Afterwards, 8 mL of deionized water was put into the above vessel, followed by ultrasonication for 30 min to acquire the homogeneous solution. Subsequently, a piece of the oxygen plasma treated CC (2×2 cm^2) was fully immersed in the above solution, and the sealed vessel was placed in an oven and reacted at 80°C for 4 h. Finally, after cooling to room temperature, the Ni-CAT@CC was taken out from the vessel, washed several times with ethanol and deionized water, and oven dried at 60°C overnight. The thickness of the Ni-CAT@CC composite film was ~ 0.342 mm.

Assembly of piezoresistive sensor based on Ni-CAT@CC

The polydimethylsiloxane (PDMS) film was bought from Hefei Keliao New Materials Co., Ltd., and the thickness of the PDMS film was 300 μm. The PDMS film was cut into a size of 3 cm × 3 cm. Two pieces of Ni-CAT@CC (2 × 2 cm^2) were placed face to face between the upper PDMS film and the lower polyimide tapes. And a copper wire was connected to one end of each Ni-CAT@CC composites film, and copper foil (1 cm × 0.5 cm) was pasted on each side to fix the copper wire. The piezoresistive sensor based on Ni-CAT@CC was completed. To monitor human behaviors, the copper foil is coated with silver paste to fix the copper wire on the surface of the Ni-CAT@CC composites film for good bonding. A 27-year-old healthy male volunteer was recruited from the Suzhou Institute of Nano-Tech and Nano-Bionics and gave informed consent prior to

testing. The Ni-CAT@CC based sensor was attached to the volunteer's skin with medical scotch tape to monitor joint movement. In the test, both ends of the senor were connected to a Keithley 2450 source meter, and the senor collected data on the computer via the Keithley 2450 source meter.

Fabrication and assembly of the soft-packaged aqueous Ni-Zn battery

The soft-packaged aqueous Ni-Zn battery was constructed based on Ni-CAT@CC composite film. Firstly, the Ni-CAT@CC composite film (2×2 cm^2) was activated by an electrochemical workstation. The activation process was carried out in 1 M KOH aqueous electrolyte via a three-electrode system, where Ni-CAT@CC composite film, Ag/AgCl electrode, and Pt wire were used as the working, reference and counter electrodes, respectively. After the cyclic voltammetry (CV) curves of the Ni-CAT@CC composite film were performed at a scan rate of 20 mV s^{-1}, 30 mV s^{-1}, and 50 mV s^{-1} for five times with the voltage window from 0 to 0.5 V, respectively, the activation of the Ni-CAT@CC composite film was completed. The soft-packaged aqueous Ni-Zn battery with a typical sandwich structure was assembled using a piece of polished Zn foil (2×2 cm^2), a piece of activated Ni-CAT@CC composite film (2×2 cm^2), glass microfiber filters as the anode, the cathode, and the separator, respectively. Then a few drops of 1 M KOH solution were added to the separator. Cu foils were bonded to the respective anode and cathode. Finally, the cell was packed using the aluminum plastic film with top and side sealing.

Characterization and measurement

Scanning electron microscopic (SEM) images were obtained using a Hitachi Regulus 8230. The microstructure of the Ni-CAT@CC composite film was measured by transmission electron microscopy (TEM, FEI Tecnai G2 F20). The surface chemical elemental compositions of Ni-CAT@CC composite film were evaluated by X-ray photoelectron spectroscopy (XPS) using a Thermo Scientific K-Alpha spectrometer. The X-ray diffractometer (XRD, D8 Advance Bruker) was used to analyze the crystal structure of the samples in the range of 2θ = 5–60°. The pressure testing system composed of universal testing machine (ZQ-990a, Dongguan Zhiqu Precision Instrument), a source meter (Keithley 2450), and a signal acquisition computer. Response time and recovery time were tested using an oscilloscope (LUCK-3, digital storage oscilloscope). The electrochemical properties of the batteries were evaluated by cyclic voltammetry (CV) and galvanostatic charge-discharge (GCD) using a multichannel electrochemical workstation (CorrTest CS3104).